

Physical aging behavior of miscible blends of poly(methyl methacrylate) and poly(styrene-*co*-acrylonitrile)

C.G. Robertson, G.L. Wilkes*

Polymer Materials and Interfaces Laboratory, Chemical Engineering Department, Virginia Polytechnic Institute and State University, Blacksburg, VA 24061-0211, USA

Received 13 January 2000; received in revised form 26 June 2000; accepted 12 July 2000

Abstract

The influence of blend composition on volume relaxation behavior was determined for miscible blends of poly(methyl methacrylate) (PMMA) and poly(styrene-*co*-acrylonitrile) (SAN). The volume relaxation rates displayed an approximately linear dependence on blend composition for all of the aging temperatures employed which were 15, 30, and 45°C below T_g . No unique behavior was observed for the blends compared to the pure polymers in terms of glass transition fragility observed by differential scanning calorimetry or the variation of density with composition. The dynamic mechanical β -relaxation process for PMMA was observed in the PMMA/SAN blends, and the intensity of the relaxation diminished with increasing SAN content. These results were contrasted with previous findings by the present authors on blends of atactic polystyrene (a-PS) with poly(2,6-dimethyl phenylene oxide) (PPO). Fragility, density, and secondary relaxation features of the PMMA/SAN and a-PS/PPO blends were influenced by the respective nature of interactions in these mixtures, and the volume relaxation rates were consistent with these characteristics. An apparent failure of time-aging time superposition was noted for PMMA due to overlapping α - and β -relaxations. © 2000 Elsevier Science Ltd. All rights reserved.

Keywords: Physical aging behavior; Miscible blends of poly(methyl methacrylate) and poly(styrene-*co*-acrylonitrile); Time-aging time superposition

1. Introduction

The nonequilibrium nature of the glassy state results in time-dependent changes in properties of amorphous materials during their use at temperatures below the glass transition temperature region, and this relaxation process is known as physical aging. Research on physical aging has recently received much attention; a survey of the literature from 1987 to 1998 reveals that over 800 publications appeared in this interim which were concerned with, to some extent, nonequilibrium glassy behavior [1]. What is remarkable given this high degree of activity in this research area is that a comprehensive understanding of the physical aging process has yet to be generated from a basic molecular standpoint. The study of the time-dependent glassy state of miscible polymer blends can provide a way of assessing the role of chemical interactions on the physical aging process, thus aiding in revealing how physical aging is influenced by intermolecular characteristics. Previous investigations by us considered the physical aging [2] and glass formation kinetics [3] of the miscible blend system composed of

atactic polystyrene (a-PS) and poly(2,6-dimethyl-1,4-phenylene oxide) (PPO). The presence of specific attractive interactions is a well-established attribute of the a-PS/PPO blends [4,5]. In contrast, blends of atactic poly(methyl methacrylate) (PMMA) with statistical copolymers of styrene and acrylonitrile (SAN) derive their miscibility by means of a “copolymer repulsion” effect which will presently be described. Investigating the aging behavior as a function of blend composition for PMMA/SAN blends can, therefore, enable a useful comparison to be made with the aging results for miscible blends of a-PS and PPO.

Mixtures of high-molecular weight polymers typically require a negative change in enthalpy with mixing, ΔH_{mix} , in order to insure that miscibility is energetically favorable [6]. Specific attractive interactions between the different blend species, which are not present in the pure polymers, can accomplish this. In blends, where at least one component is a random copolymer, miscibility does not need to be a result of specific interactions but rather the necessary negative value of the Flory–Huggins interaction parameter, χ , can be derived from by what is known as the “copolymer repulsion effect” [7–13]. As an example, the interaction parameter can be expressed as follows [7,8]: for a blend of a homopolymer (A) made up of type 1 segments and a

* Corresponding author. Tel.: +1-540-231-5498; fax: +1-540-231-9022.
E-mail address: gwilkes@vt.edu (G.L. Wilkes).

random copolymer (B) composed of molecular units 2 and 3:

$$\chi_{A,B} = b\chi_{1,2} + (1 - b)\chi_{1,3} - b(1 - b)\chi_{2,3} \quad (1)$$

The variable b denotes the mole fraction of the type 2 repeat unit in the copolymer, and the χ subscripts indicate which two molecular units are associated with each binary interaction parameter. A negative interaction parameter between the homopolymer and the copolymer ($\chi_{A,B}$) can be obtained for a range of copolymer compositions even if the interaction parameters between all of the different segments are all greater than zero. This can occur if less attraction exists between the chemically linked copolymer units 2 and 3 than is present between either of these units and the homopolymer unit 1:

$$0 < \chi_{1,2} < \chi_{2,3} \quad \text{and} \quad 0 < \chi_{1,3} < \chi_{2,3} \quad (2)$$

with the magnitudes of the inequalities dictated by the copolymer composition, b .

Poly(methyl methacrylate) is not miscible with either polystyrene or polyacrylonitrile but yet it can form miscible blends with poly(styrene-*co*-acrylonitrile) for statistical copolymers with approximately 9–35 wt.% acrylonitrile due to the copolymer repulsion effect [11,13]. The term “repulsion effect” is really a misnomer; all of the interactions are attractive but some pair–pair interactions are invariably more attractive than others.

Study of the PMMA/SAN blend system by ^{13}C NMR was performed by Feng et al. [14]. These authors suggested that miscibility was not a consequence of the copolymer repulsion effect but rather due to attractive interactions between the carbonyl of PMMA and the phenyl side group on the polystyrene repeat unit of the SAN copolymer. The attractive interactions between PMMA and SAN are quite weak, however, and cannot alone explain the miscibility between PMMA and SAN which is observed despite the fact that miscible blends of PMMA cannot be formed with either polystyrene or polyacrylonitrile. Kwei et al. [15] noted evidence for interaction involving the carbonyl group of PMMA in mixtures of PMMA and SAN by means of infrared absorption measurements, but they concluded that only ca. 3% of the PMMA repeat units contributed to the shifted carbonyl band. The result of Feng and coworkers that some attractions exist between the phenyl group of the SAN copolymer and the carbonyl of PMMA is not being refuted. What is being stated is that the predominant opinion concerning the PMMA/SAN blends is that miscibility is a result of the copolymer repulsion effect [11–13,16], and we are also proponents of this view.

The goal of this investigation was to characterize the sub- T_g volume relaxation as a function of composition for blends of PMMA and SAN. This research was initiated in order to contrast the aging behavior for the a-PS/PPO and PMMA/SAN blend systems in view of their differences in the nature of interactions and miscibility. A few physical aging studies of the PMMA/SAN blends have been reported in the literature. Kwei and coworkers [15] performed a limited

examination of enthalpy relaxation/recovery as part of a comprehensive study of the physical properties of PMMA/SAN blends. Aging was considered by Mijovic et al. [17–21] for blends of PMMA and SAN by assessing changes in both enthalpy and stress relaxation response. Changes in stress relaxation due to the physical aging process were also recently investigated for the PMMA/SAN blend system by Cowie et al. [22]. Further details of these studies will be included later where appropriate. None of these prior studies, however, characterized volume relaxation behavior of PMMA/SAN polymer blends which represents the focus of this present communication.

2. Experimental details

2.1. Preparation and characterization of blends

Atactic poly(methyl methacrylate) (PMMA) and a statistical copolymer of styrene and acrylonitrile containing 25 mol.% acrylonitrile (SAN) were melt blended for 15 min at 170°C and 70 rpm in a Brabender (Model 5501) melt mixer using a nitrogen purge. The atactic PMMA was obtained from Aldrich Chemical Company (Cat. #44,574-6) and has a M_w of approximately 350,000 g/mol. The SAN material is reported to have an approximate M_w of 165,000 g/mol and this polymer was also obtained from Aldrich (Cat. #18,285-0). The polymer materials were dried under vacuum conditions at 70°C before blending. Blends with compositions of 25, 50, and 75 wt.% SAN were made. The nomenclature PMMA/SANXX will be used to describe each blend where XX represents the SAN content in units of wt.%. Films of approximate thickness 0.2 mm were compression molded from PMMA, SAN, and the blends at 175°C. Glass transition responses were measured by differential scanning calorimetry (DSC) for samples which were freshly quenched into the glassy state at a rate of 200°C/min (see Section 2.4). The midpoint, or inflection, glass transition temperature, T_g , was measured and an indication of the transition breadth was also obtained for each material. Specific volume data were assessed at 23°C using a model AccuPyc 1330 pycnometer manufactured by Micromeritics for samples which were freshly quenched from $T_g + 30^\circ\text{C}$ (rapidly quenched by placing samples between two steel plates at room temperature).

2.2. Volume relaxation measurements

Volume relaxation experiments were performed on the neat materials and the blends using a mercury dilatometry apparatus constructed by Shelby [23]. Compression molded samples of approximate weight 6 g (dimensions ca. $1.0 \times 1.5 \times 4 \text{ cm}^3$) were sealed in the glass bulbs of the dilatometers. The dilatometers were then filled with mercury and de-gassed under vacuum. Prior to each run, the encased sample was equilibrated at 30°C above T_g using a Fisher

Scientific 1006D oil bath and subsequently quenched to 0°C using an ice bath. The dilatometer and enclosed sample was then placed back into the oil bath after the bath was cooled to the desired aging temperature of 15, 30, or 45°C below T_g . Isothermal annealing was then performed for approximately four days while volume changes were assessed from the height of the mercury in the capillary of the glass dilatometer using a linear voltage differential transducer. Three runs were conducted at the undercooling of 30°C in order to provide an indication of the measurement error. Experimental details beyond those given here can be found elsewhere [2,23].

2.3. Creep compliance measurements

The influence of physical aging on small-strain tensile creep compliance behavior was assessed for neat PMMA during isothermal aging at $T_a = T_g - 30^\circ\text{C}$. Each sample was cut and tested after a piece of PMMA film was rapidly quenched from $T_g + 30^\circ\text{C}$ to well below T_g by placing it between two steel plates at room temperature. Using the procedure established by Struik [24], the small-strain creep response was probed after aging times of 1.5, 3, 6, 12, and 24 h. A Seiko thermal mechanical analyzer (model TMA 100) was used to test the samples which had a length of 25 mm length, thickness of 0.2 mm, and a width of 3 mm (approximate dimensions). Creep measurements on the blends were not performed because an apparent failure of time–aging time superposition was noted for pure PMMA (see Section 3).

2.4. Differential scanning calorimetry

The kinetic nature of the glass transition was probed using differential scanning calorimetry (DSC). A properly calibrated Perkin Elmer DSC7 was used, and the sample and reference cells of this instrument were constantly kept under a nitrogen purge during measurements and while the instrument was idle. The temperature was calibrated using tin and indium, and the heat flow was calibrated using indium. Particular care was taken to insure that changes in the instrument baseline did not occur during the measurements. Each sample weighing approximately 10 mg was cooled in the calorimeter from $T_g + 50^\circ\text{C}$ to $T_g - 50^\circ\text{C}$ at a fixed rate of 1, 3, 10, 30, 60, or 100°C/min and then measurements were made as the sample was then heated back to $T_g + 50^\circ\text{C}$ at 10°C/min. Three samples were tested for each cooling rate, and this testing was performed for all of the blend compositions. Fictive temperature calculations were conducted on the heating scans using the Perkin Elmer analysis software.

2.5. Dynamic mechanical analysis

Dynamic mechanical measurements were made under tension using a Seiko DMS 210. The samples had the approximate dimensions of $0.2 \times 5 \times 10 \text{ mm}^3$. The testing was performed on freshly quenched samples which were

generated by annealing films at a temperature of $T_g + 30^\circ\text{C}$ for 10 min and then quenching them to well below T_g by placing them between steel plates at room temperature. The testing procedure involved a heating rate of 2°C/min, a nitrogen purge, and a frequency of 1 Hz. The dynamic mechanical response was assessed accordingly for each material from approximately -140°C to above the α -relaxation temperature region.

2.6. Thermal contraction measurements

A model TMA 100 Seiko thermal mechanical analyzer was used to measure linear thermal contraction during cooling the PMMA, SAN, and PMMA/SAN50 materials at 1°C/min from $T_g + 20^\circ\text{C}$ to 50°C. The samples possessed the following approximate dimensions: length of 25 mm, thickness of 0.2 mm, and width of 3 mm. A very small tensile load was maintained during testing but this did not induce any significant amount of creep as was verified by holding the sample under tension for 15 min at $T_g + 20^\circ\text{C}$. Four samples were tested for each material and density measurements were made on the samples after the cooling runs were all performed. The four samples were cut up and combined for testing at 23°C using the Micromeritics AccuPyc 1330 pycnometer in order to transform the relative density behavior assessed for the isotropic samples during cooling into actual volume versus temperature curves.

3. Results and discussion

The isothermal decay of volume in the glassy state was assessed as a function of both aging temperature and blend composition, and the information gained from this experimentation will be presented and discussed. Specifically, an attempt to gain an understanding of the volume relaxation results will be undertaken based upon supporting data concerning the influence of blend composition on: (1) initial density prior to aging; (2) kinetics of the glass formation process; and (3) intensity of secondary relaxation processes. This will allow a comparison of the volume aging behavior of the PMMA/SAN blends with the results which were previously reported for the a-PS/PPO system [2,3].

3.1. Physical aging results

Dilatometry was used to follow decreases in volume during sub- T_g annealing for PMMA, SAN, and their blends. The aging temperature, T_a , values employed were 15, 30, and 45°C below T_g . The inflection DSC glass transition temperature, T_g , values were measured during heating at 10°C/min immediately following a quench into the glassy state at 200°C/min. The glass transition temperature did not vary substantially with blend composition as is illustrated in Fig. 1a. Specific volume data are given versus composition in Fig. 1b, and discussion of these results is reserved for later. Some representative volume relaxation results

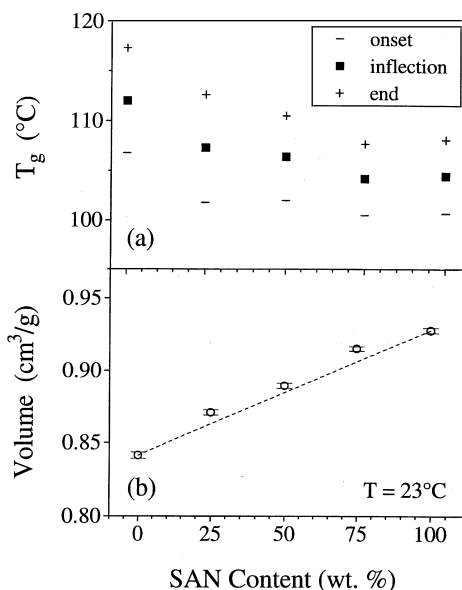


Fig. 1. (a) DSC glass transition temperature results and (b) room temperature specific volume data.

obtained at $T_g - 30^\circ\text{C}$ are provided by Fig. 2. To quantify the volume aging behavior (isothermal and isobaric) and enable comparisons to be made, each volume relaxation rate, b_V , was determined according to the following [24,25]:

$$b_V = -\frac{1}{V} \frac{dV}{d \log t_a} \quad (3)$$

The influences of composition and undercooling ($T_g - T_a$) on volume relaxation rate can be observed from Fig. 3. Volume relaxation rates increased in an essentially linear manner with regard to SAN content for both the undercoolings of 15 and 30°C . For the aging temperature of $T_g - 45^\circ\text{C}$, b_V was noted to be nearly independent of

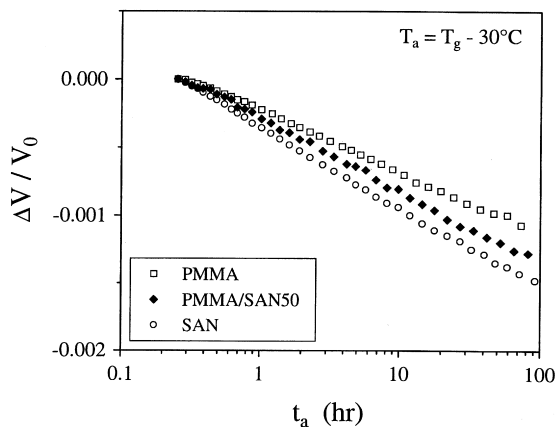


Fig. 2. Typical volume relaxation results for aging performed at $T_g - 30^\circ\text{C}$. An aging time of 0.25 h was used as the reference for determining volume differences (ΔV values). The negative slope of each data set represents the volume relaxation rate, b_V , and data points between 0.6 and 80 h (approximately) were used in the rate determination.

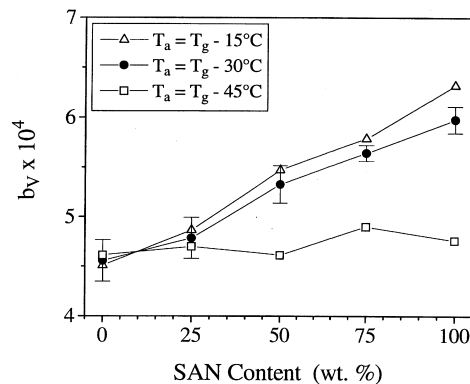


Fig. 3. Variation of volume relaxation rate with composition and aging temperature.

blend composition. Explanation of the observed volume relaxation rate trends will be undertaken later.

The volume relaxation trends presented here are, in general, comparable with the results of the previous studies which investigated enthalpy relaxation/recovery for the PMMA/SAN blends. Kwei and coworkers [15] annealed PMMA/SAN samples for 88 h at 85°C (approximately $T_g - 20^\circ\text{C}$ for the neat polymers as well as the blends) and noted that the degree of enthalpy recovery was essentially constant with respect to composition. These enthalpy recovery data were unlike the volume relaxation results at a similar undercooling of $T_g - 15^\circ\text{C}$ presented in this communication in that the volume relaxation rates were found to increase with SAN content. Physical aging was only a minor component of this previous study by Kwei et al., and measurements of the degree of enthalpy recovery as a function of $\log(\text{aging time})$ were not made to assess enthalpy aging rates. The limited enthalpy recovery data acquired for annealing at 85°C for 88 h did provide an indication that the blends displayed relaxation/recovery characteristics which were intermediate to the responses for pure PMMA and SAN. The present volume relaxation study supports this general result. A more comprehensive examination of enthalpy relaxation/recovery was later undertaken for the PMMA/SAN blend system by Mijovic et al. [18]. The conclusions reached by these researchers are quite consistent with the volume relaxation results presented here; the decay of enthalpy with $\log(\text{aging time})$ was essentially intermediate for the blends compared to the pure components and increased with SAN content at $T_g - 20^\circ\text{C}$ and $T_g - 35^\circ\text{C}$ while the rate of enthalpy relaxation was independent of composition at $T_g - 50^\circ\text{C}$. Therefore, these new dilatometric findings reinforce the trends present in published enthalpy relaxation data.

At the outset of this study, the intention was to characterize the mechanical aging of the PMMA/SAN materials. This turned out to be problematic due to concern for whether Struik's [24] time-aging time superposition was valid for PMMA and, as an extension, for blends of PMMA with SAN. Small-strain creep compliance response was measured

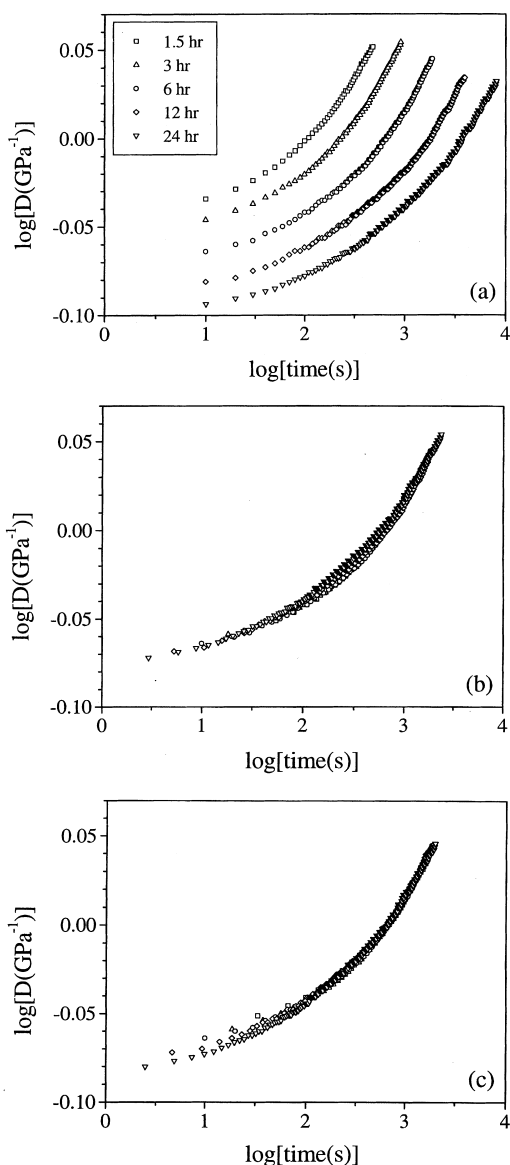


Fig. 4. (a) Creep compliance behavior for PMMA following aging at $T_g - 30^\circ\text{C}$ for the indicated aging times. (b) Attempt to generate a master curve via horizontal and vertical shifting in order to superimpose the entire data set for each aging time. (c) Attempt to superimpose the long time portion of the creep data. The reference response used during the superposition attempts was that obtained at an aging time of 6 h.

for PMMA following aging at 82°C ($T_g - 30^\circ\text{C}$) for aging times of 1.5, 3, 6, 12, and 24 h. Typical results are presented in Fig. 4a. An attempt to superimpose all of the creep data by horizontal and vertical shifting was performed with the outcome represented by the apparent master curve shown in Fig. 4b. Although a fair master curve could be formed, some question concerning the applicability of time–aging time superposition remained; the creep data points in the middle of this apparent master curve (Fig. 4b) do not superimpose well. When only superposition of the long time portions of the creep data was performed, excellent reduction of the long time data was possible as is illustrated in Fig. 4c. However, the

short time response appeared to display a dependence on aging time not accounted for by the horizontal and vertical shifting necessary to superimpose the long time data. This behavior was observed for all three PMMA samples tested under these conditions.

The apparent failure of the superposition for the PMMA creep data is consistent with creep studies performed by Read and coworkers [26,27] on polymers with overlapping primary and secondary mechanical relaxations. When two distinct relaxations both exert some influence on the data in the experimental window accessible by the mechanical measurements, it is anticipated that thermorheological complexity will be the result. An intense secondary relaxation is a characteristic feature of PMMA, and this relaxation significantly overlaps with the α -relaxation (glass transition). This is a well-established feature of the dynamic mechanical behavior of PMMA [28]. This relaxation, albeit reduced in magnitude, is also present in the PMMA/SAN blends as is illustrated in Fig. 5. The secondary relaxations for the blends will be further discussed later. Within the nonequilibrium regime, the typical effect of aging on the α -relaxation of an amorphous polymer is a shift of the high frequency (low temperature) portion of the segmental relaxation time response to longer times. In general, the temperature/frequency location of a secondary relaxation appears to be unaffected by the aging process [27,29,30]. There is some debate concerning whether the intensity of a secondary relaxation diminishes with physical aging or whether, instead, it is actually the high-frequency tail of the α -relaxation dispersion which is affected by aging [29–33]. What is quite clear is that the physical aging process can influence the α - and β -relaxations very differently. Therefore, when the primary and secondary relaxation processes overlap in the temperature and time regions where mechanical aging studies are performed, failure of the time–aging time superposition can result.

Both failure and success of the time–aging time superposition principle as applied to PMMA has been observed. Failure of time–aging time superposition has been clearly established for the small-strain creep behavior of PMMA at

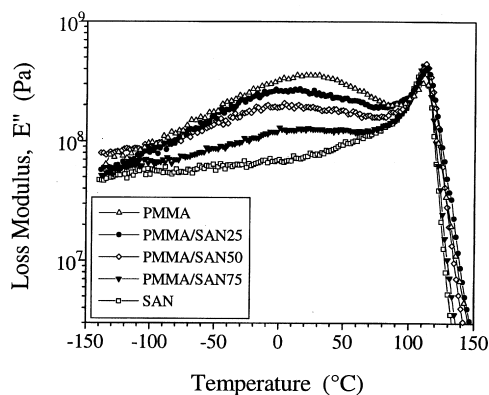


Fig. 5. Loss modulus data obtained at a heating rate of $2^\circ\text{C}/\text{min}$ using a testing frequency of 1 Hz.

40 and 60°C by McKenna and Kovacs [34], but these researchers found that decent superposition of creep data could be performed at 80°C, unlike the present study which indicated questionable superposition at a similar aging temperature of 82°C ($T_g - 30^\circ\text{C}$). An examination of mechanical aging of the PMMA/SAN blend system has been performed by Mijovic and coworkers [17,20,21] as well as Cowie et al. [22] and these stress relaxation studies indicated no evidence of failure of time–aging time superposition for any of the neat materials or blends. This successful mechanical data reduction observed in the study by Cowie et al., is not surprising given the relatively close proximity of the aging temperatures to the glass transition temperature. The investigated undercoolings were all less than 30°C, and the influence of the secondary relaxation on the experimentally accessible creep response becomes diminished relative to the α -relaxation contribution as temperature is increased. The complete success of superposition noted in the study by Mijovic et al. is unexpected, however, because these researchers utilized aging temperatures down to $T_g - 50^\circ\text{C}$ which, for neat PMMA, is an aging temperature in close proximity to 60°C where McKenna and Kovacs found clear failure of time–aging time superposition for this material. An in-depth study of the applicability of the time–aging time reduction scheme to mechanical data for glassy blends of PMMA and SAN, although certainly warranted, is outside the scope of this present investigation. If Struik's reduction principle is invalid in a general sense for pure PMMA and for PMMA/SAN blends, then mechanical aging rates cannot be adequately compared with the goal of determining the influences of composition and temperature on mechanical aging behavior.

3.2. Interpretation of aging results and comparison with a-PS/PPO blends

An earlier study of the miscible blend system comprised of a-PS/PPO revealed that the compositional variation of glassy density, fragility, and secondary relaxation intensity provided insight into physical aging results for these blends [2,3]. These characteristics were also investigated for the PMMA/SAN blend system of current interest. This information will be employed in order to understand the noted variation of volume relaxation rate with composition and aging temperature for the PMMA/SAN system, and this will further enable the aging behavior of the a-PS/PPO and PMMA/SAN blend systems to be contrasted.

Quenching an amorphous polymer into the glassy state captures a certain amount of free volume, which can further decrease during physical aging. The free volume which is present prior to aging controls, in addition to other chemical and structural features, the initial degree of mobility at a given temperature in the glassy state. This initial mobility can influence the subsequent rate of volume relaxation during annealing due to the self-limiting character of the physical aging process. Self-limitation describes the

circular process wherein mobility enables the structural rearrangements necessary for a reduction in the volume toward the equilibrium state, and this densification serves to further retard the mobility. Accordingly, the initial amount of free volume, which is induced by the quenching process, can influence the rate of volume relaxation during aging.

It was observed that unaged density characteristics could help explain the compositional dependence of volume relaxation rates for the a-PS/PPO blend system aged at undercoolings of 15 and 30°C. Negative deviation in freshly quenched specific volumes was observed for the a-PS/PPO blends compared to additivity and a comparable deviation was also noted from the b_V versus composition data at $T_g - 15^\circ\text{C}$ and $T_g - 30^\circ\text{C}$. The volume relaxation rates obtained for aging the a-PS/PPO system at $T_g - 60^\circ\text{C}$ were linear with composition, however, and this will be addressed later during consideration of the effects of secondary relaxations on aging rates. In contrast to the excess volume characteristics in the glassy state for blends of a-PS and PPO, the variation of specific volume with composition for freshly quenched samples of the PMMA/SAN materials displayed an essentially linear trend as was shown earlier in Fig. 1b. A linear dependence of volume relaxation rate on SAN content was also obtained for all of the undercoolings employed in this PMMA/SAN aging study (Fig. 3), which was consistent with the specific volume data prior to aging. A linear dependence of b_V on composition was noted for the PMMA/SAN blends at the undercoolings of 15, 30, and 45°C, but the slope of the dependence varied with undercooling. This feature of the data will be further discussed later.

Previous research on the a-PS/PPO blend system indicated a close tie between the glass formation kinetics and excess volumes in the glassy state for the blends. The variation of the initial glassy density (induced by a quench from above T_g) with blend composition is influenced by the relative kinetics of glass formation for the miscible blends compared to the behavior observed for the pure components. The negative excess volumes observed for the a-PS/PPO blends in the glassy state are not present at temperatures in the liquid state [3,35]. The negative excess volumes for the blends in the glassy state are due to the fact that the specific interactions between the a-PS and PPO components heighten the fragility (cooperativity) of the blends compared to pure a-PS and PPO [3]. Fragility is essentially a normalized activation energy (normalized by $\ln(10)RT_g$) determined at a reference glass transition temperature [36]. Volume contraction with mixing is typically inferred from glassy state density versus composition data even though mixing of the amorphous polymers occurs in the liquid state above the highest component T_g . This proved to be an inappropriate approach for the case of the a-PS/PPO blends where it was clear that the negative ΔV_{mix} values noted in the glassy state were caused by kinetic, rather than thermodynamic, effects. This proved that the presence of specific interactions caused the increased density for the blends compared to

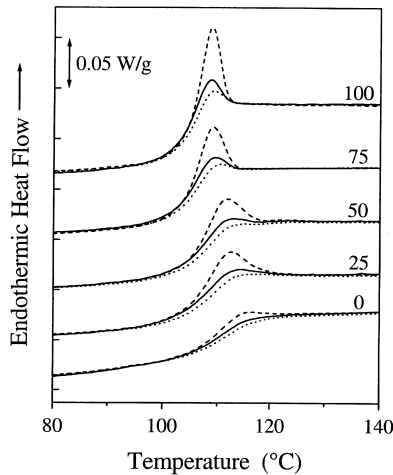


Fig. 6. DSC heating traces obtained during heating at 10°C/min following cooling at 1°C/min (dashed lines), 10°C/min (solid lines), and 100°C/min (dotted lines). The numbers represent the SAN content in wt.%.

additivity in the glassy state which in turn affected the subsequent volume relaxation rate behavior at $T_g - 15^\circ\text{C}$ and $T_g - 30^\circ\text{C}$.

It was mentioned previously that the PMMA/SAN blends do not possess attractive interactions between the components comparable to those present between a-PS and PPO in their miscible mixtures. The positive deviation of fragility from additivity due to the interactions between a-PS and PPO in the blends caused the negative deviation in the specific volume versus PPO content data in the glassy state. It is informative to consider the fragility characteristics of the PMMA/SAN blends and compare them to the glass formation kinetics of the neat polymers. It is not the intention of the authors to reiterate the details of the fragility concept in this present communication; a detailed explanation is provided in other publications [3,36–38].

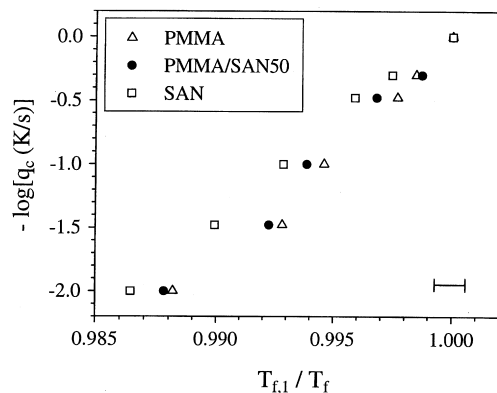


Fig. 7. Relationship between the cooling rate (q_c) and the fictive temperature assessed from the DSC heating scans at 10°C/min. The fictive temperature associated with the cooling rate of 1°C/min, $T_{f,1}$, is used as a normalization constant for each material. The magnitude of a typical error bar associated with the normalized fictive temperature data is given in the plot.

Fragilities were not assessed from dynamic mechanical α -relaxation data of the PMMA/SAN materials because of concern for the convoluting influence of the intense secondary relaxation which overlaps the α -relaxations of pure PMMA and the blends (Fig. 5). However, consideration of DSC heating scans through the glass transition region can provide quantitative information about glass transition kinetics if the cooling rate employed just prior to the heating scans (fixed heating rate) is systematically varied [3,39]. Recent work on amorphous linear polymers illustrated that a measure of fragility determined in such a manner using DSC was essentially equivalent to the respective fragility assessed from the segmental dynamics of the α -relaxation using mechanical and dielectric spectroscopies [40].

Typical DSC results for the PMMA/SAN materials are indicated in Fig. 6 as a function of blend composition. A value of fictive temperature [41–43], T_f , was determined from each heating trace using the Perkin–Elmer software. The relationship between cooling rate, q_c , and fictive temperature is shown in Fig. 7 for PMMA, SAN, and the PMMA/SAN50 blend. The slope of each data set plotted in the manner indicated in Fig. 7 directly yields a value of fragility, m . Fragility is generally expressed as the T_g -normalized dependence of relaxation time, τ , according to:

$$m = \frac{d \log(\tau)}{d(T_g/T)} \quad (4)$$

Information concerning the variation of fragility with SAN content was generated from the DSC data, resulting in the essentially linear trend indicated in Fig. 8. The fragility value determined for PMMA is comparable to other literature results [36,44] which serves to verify the merit of the data presented herein.

The fragility characteristics of the PMMA/SAN blends are linearly intermediate to the fragility characteristics of neat PMMA and SAN. It is expected, therefore, that the variation of specific volume with composition should be similar for the liquid and glassy states, unlike the a-PS/PPO results. Thermal contraction experiments were carried

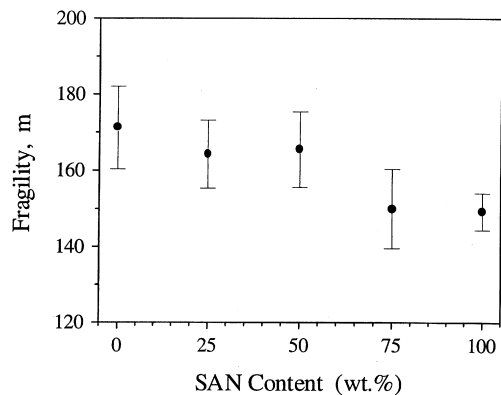


Fig. 8. Influence of blend composition on the fragility determined from the DSC data.

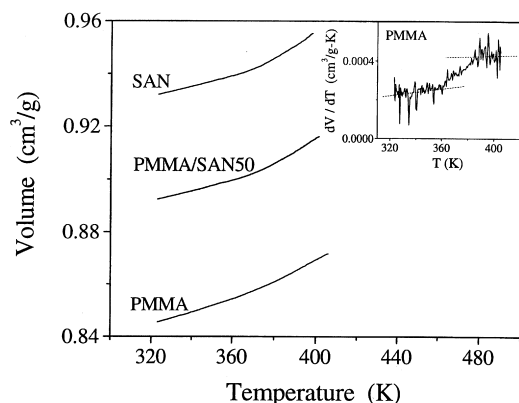


Fig. 9. Thermal contraction responses assessed during cooling at 1°C/min.

out during cooling at 1°C. As can be seen from the data presented in Fig. 9, the cooling curve for the 50/50 blend is essentially intermediate to the data of PMMA and SAN in both the liquid and glassy states. Because strong attractive interactions are not present between PMMA and SAN in the blends, no increased fragility behavior was noted for the blends compared to the pure component responses which resulted in the maintenance of the liquid state excess volume for the 50/50 blend upon cooling into the nonequilibrium glassy state. This observation is in contrast to the behavior of the a-PS/PPO blend system [3]. Glass transition temperatures associated with the linear dilatometry results cannot be quantitatively compared to the DSC data due to difficulty in assigning transition temperatures for the volume–temperature data (for example, see inset of Fig. 9).

Characterization of secondary relaxation intensity as a function of blend composition can allow the development of some understanding concerning changes in b_V versus blend composition trends which occur as aging temperature is varied. It was observed that the a-PS/PPO blends possessed secondary relaxations in the vicinity of the β -relaxation for neat atactic polystyrene [2]. The intensity of the relaxation, however, did not diminish in a simple manner with increasing PPO content due to additional motion of the PPO which occurred in cooperation with the a-PS secondary dispersion. The fact that the variation of b_V with composition changed from a trend characterized by negative deviation from additivity at $T_g - 30^\circ\text{C}$ to a linear trend at $T_g - 60^\circ\text{C}$ was attributed to these secondary relaxation characteristics. It was discovered that an indication of the change in mobility in going from one glassy temperature to another could be obtained by a ratio of the loss modulus values at these two temperatures for a fixed set of testing conditions. The variation of this loss modulus ratio with blend composition was remarkably comparable to the compositional dependence of a similar ratio determined for volume relaxation rate for the a-PS/PPO blend system. This suggested that a dynamic mechanical spectrum could provide some prediction of relative volume relaxation rates

of an amorphous polymer for two substantially different glassy temperatures (temperature difference of 30°C).

A link between the temperature dependence of the isochronal dynamic mechanical $\tan \delta$ and the shape of the volume relaxation rate versus temperature curve was first noted by Struik [45] using data for numerous amorphous polymers. This connection was also observed from the previous research reported by us on the a-PS/PPO blends and, as will be shown, from the present work on the PMMA/SAN materials. While this connection may be a decent qualitative or even semi-quantitative tool, it is worthwhile to address a few caveats. The characteristic time scale for relaxation in the nonequilibrium glassy state increases as the aging process proceeds; this is the nonlinear feature of physical aging [46]. Connecting volume relaxation rates to mobility inferred from dynamic loss modulus at a constant frequency is somewhat tenuous. Also, activation energies for localized secondary relaxations are small compared to those associated with the cooperative α -relaxations such that the shape of the isochronal loss modulus–temperature spectrum varies with the testing frequency.

The secondary relaxation process for PMMA was observed in the PMMA/SAN blends (see Fig. 5). Unlike the a-PS/PPO dynamic mechanical results, the secondary relaxation intensities of the PMMA/SAN blends decreased with decreasing PMMA content in a fashion consistent with the fact that only motion of PMMA was responsible for the relaxation. The ratio of properties at $T_g - 15^\circ\text{C}$ to those at $T_g - 45^\circ\text{C}$ was determined for the properties of loss modulus and volume relaxation rate which were measured for the PMMA/SAN system. The results are plotted in Fig. 10. It can be concluded from the similarity of the loss modulus and b_V ratio parameters that the temperature dependence of the volume relaxation rates (Fig. 3) was related to the systematic dependence of secondary relaxation intensity on blend composition.

Comparison of the two blend systems in this paper has enabled the development of an informative picture of the physical aging process for miscible blends. Contrasting the PMMA/SAN and a-PS/PPO blend systems allowed some

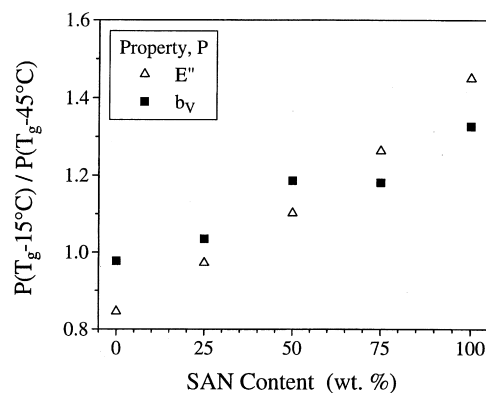


Fig. 10. Ratio of property value at $T_g - 15^\circ\text{C}$ to value at $T_g - 45^\circ\text{C}$ for the properties of volume relaxation rate and loss modulus (1 Hz, heating at 2°C, freshly quenched sample).

understanding of the role of attractive interactions on the volume relaxation process to be gained. It must be pointed out that these two blend systems have an important difference which is beyond their distinction concerning the nature of interactions. The glass transition temperatures of PMMA and SAN are quite similar while the glass transition temperature of PPO is approximately 100°C higher than that of a-PS. Concentration fluctuations in the a-PS/PPO blends, therefore, introduce more heterogeneity with regard to mobility than is caused by local variations in composition for the PMMA/SAN blends. It was shown, however, that the presence of concentration fluctuations was not responsible to any significant extent for the observed trends in volume relaxation rate for the a-PS/PPO blend system [2]. Although the PMMA/SAN and a-PS/PPO systems do not provide a perfect basis for comparison, progress towards understanding the influence of intermolecular features on the glass formation and volume relaxation processes was made by their study nonetheless.

4. Conclusions

The effects of aging temperature and composition on volume relaxation rate, b_v , was investigated for blends of PMMA and SAN. Volume relaxation rates were found to be essentially linear with composition for the aging temperatures of 15, 30, and 45°C below T_g . Fragility (from calorimetry) and unaged density in the glassy state were both linear with SAN content in the blends which helped to explain the noted dependence of volume relaxation rate on composition. The secondary relaxation process for PMMA was observed in the blends and decreased systematically in intensity as the amount of PMMA was decreased in the blends. The noted effect of aging temperature on the volume relaxation rates was attributed to the influence of the secondary relaxation characteristics. All of the above observations were consistent with the lack of attractive interactions between the components in these blends. The results of this study were contrasted with data for the a-PS/PPO blend system, and a better understanding of the role of interactions on volume relaxation emerged as a result.

Acknowledgements

A research fellowship supplied by Phillips Petroleum and a summer fellowship provided by Eastman Chemical are greatly appreciated.

References

- [1] ISI Science Citation Index, search: physical aging, physical ageing, volume relaxation, or enthalpy relaxation.

- [2] Robertson CG, Wilkes GL. Physical aging behavior of miscible blends containing atactic polystyrene and poly(2,6-dimethyl-1,4-phenylene oxide). *Polymer* 2000 (in press).
- [3] Robertson CG, Wilkes GL. Glass formation kinetics for miscible blends of atactic polystyrene and poly(2,6-dimethyl-1,4-phenylene oxide). Submitted for publication.
- [4] Feng H, Feng Z, Ruan H, Shen L. *Macromolecules* 1992;25:5981.
- [5] Goh SH, Lee SY, Zhou X, Tan KL. *Macromolecules* 1999;32:942.
- [6] Barlow JW, Paul DR. *Polym Engng Sci* 1981;21:985.
- [7] Kambour RP, Bendler JT, Bopp RC. *Macromolecules* 1983;16:753.
- [8] ten Brinke G, Karasz FE, MacKnight WJ. *Macromolecules* 1983;16:1827.
- [9] Paul DR, Barlow JW. *Polymer* 1984;25:487.
- [10] Woo EM, Barlow JW, Paul DR. *Polymer* 1985;26:763.
- [11] Suess M, Kressler J, Kammer HW. *Polymer* 1987;28:957.
- [12] Cowie JMG, Lath D. *Makromol Chem Macromol Symp* 1988;16:103.
- [13] Nishimoto N, Keskkula H, Paul DR. *Polymer* 1989;30:1279.
- [14] Feng H, Ye C, Feng Z. *Polym J* 1996;28:661.
- [15] Naito K, Johnson GE, Allara DL, Kwei TK. *Macromolecules* 1978;11:1260.
- [16] Higashida N, Kressler J, Inoue T. *Polymer* 1995;36:2761.
- [17] Mijovic J, Devine ST, Ho T, Appl J. *Polym Sci* 1990;39:1133.
- [18] Mijovic J, Ho T, Kwei TK. *Polym Engng Sci* 1989;29:1604.
- [19] Ho T, Mijovic J. *Macromolecules* 1990;23:1411.
- [20] Ho T, Mijovic J, Lee C. *Polymer* 1991;32:619.
- [21] Mijovic J, Ho T. *Polymer* 1993;34:3865.
- [22] Cowie JMG, McEwen IJ, Matsuda S. *Soc. J Chem Soc Faraday Trans* 1998;94:3481.
- [23] Shelby MD. PhD dissertation, Virginia Polytechnic Institute and State University, 1996.
- [24] Struik LCE. *Physical aging in amorphous polymers and other materials*. New York: Elsevier, 1978.
- [25] Greiner R, Schwarzl FR. *Rheol Acta* 1984;23:378.
- [26] Read BE, Tomlins PE, Dean GD. *Polymer* 1990;31:1204.
- [27] Read BE. *J Non-Cryst Solids* 1991;131–133:408.
- [28] McCrum NG, Read BE, Williams G. *Anelastic and dielectric effects in polymeric solids*. New York: Dover Publications, 1967 (p. 238–55).
- [29] Struik LCE. *Polymer* 1987;28:57.
- [30] Diaz-Calleja R, Ribes-Greus A, Gomez-Ribelles JL. *Polymer* 1989;30:1433.
- [31] Muzeau E, Vigier G, Vassoille R. *J Non-Cryst Solids* 1994;172–174:575.
- [32] Johari GP. *J Chem Phys* 1982;77:4619.
- [33] Guerdoux L, Marchal E. *Polymer* 1981;22:1199.
- [34] McKenna GB, Kovacs AJ. *Polym Engng Sci* 1984;24:1138.
- [35] Zoller P, Hoehn HH. *J Polym Sci: Polym Phys Ed* 1982;20:1385.
- [36] Böhm R, Ngai KL, Angell CA, Plazek DJ. *J Chem Phys* 1993;99:4201.
- [37] Roland CM, Ngai KL. *J Non-Cryst Solids* 1994;172–174:868.
- [38] Roland CM, Ngai KL. *Macromolecules* 1991;24:5315.
- [39] Hodge IM. *J Non-Cryst Solids* 1994;169:211.
- [40] Robertson CG, Santangelo PG, Roland CM. *J Non-Cryst Solids* 2000 (in press).
- [41] Tool AQ. *J Am Ceram Soc* 1946;29:240.
- [42] Tool AQ. *J Res Natl Bur Stand* 1946;37:73.
- [43] Hutchinson JM. *Prog Polym Sci* 1995;20:703.
- [44] Hodge IM. *Macromolecules* 1983;16:898.
- [45] Struik LCE. *Polymer* 1987;28:1869.
- [46] Kovacs AJ. *Fortschr Hochpolym-Forsch* 1964;3:394.